Int. J. Electrochem. Sci., 12 **(2017)** 6232 – 6244, doi: 10.20964/2017.07.03

International Journal of
ELECTROCHEMICAL
SCIENCE
www.electrochemsci.org

Corrosion Inhibition of Mild Steel in Sulfuric Acid Solution by Houttuynia Cordata Extract

Xingwen Zheng[1, 2,*], *Min Gong*[2], *Qiang Li*[1]

[1] School of Chemical and Environmental Engineering, Sichuan University of Science & Engineering, Zigong 643000, China
[2] Key Laboratory of Material Corrosion and Protection of Sichuan Province, Zigong 643000, China
[*]E-mail: zxwasd@126.com

Received: 28 February 2017 / *Accepted:* 21 April 2017 / *Published:* 12 June 2017

The inhibition performance and mechanism of Houttuynia cordata extract (HCE) for the corrosion of mild steel in 0.5 M H_2SO_4 were investigated using weight loss method, electrochemical measurements and scanning electron microscope (SEM). The results revealed that HCE was an effective mixed-type inhibitor with a predominantly cathodic action for mild steel in 0.5 M H_2SO_4 solution, its inhibition efficiency increases with the increase of the concentration of HCE, and when the concentration of HCE reaches 0.75 g/L, the inhibition efficiency is up to 90 % at 298 K. The adsorption of HCE on steel surface obeyed Langmuir adsorption isotherm, thus the thermodynamic and kinetic parameters were calculated and discussed.

Keywords: Houttuynia cordata; Mild steel; H_2SO_4; Corrosion inhibitor; Adsorption.

1. INTRODUCTION

Corrosion inhibitor as an effective additive has been widely applied to restrain the corrosion of metal in acid media. A large number of various synthetic compounds, whose molecular structures contain unsaturated bonds or plane conjugated systems as well as heteroatoms such as nitrogen, oxygen, sulfur, phosphorus [1-4], have been reported as corrosion inhibitors, and exhibit good inhibition performance. However, most of them are highly toxic to living organisms and environment [5-8]. Due to increasing environmental protection awareness and strict environmental protection regulations, plant extracts as corrosion inhibitor have attracted extensive attention due to their environment-friendliness, low cost and renewability, and, in recent years, hundreds of plant extracts have been reported as inhibitors for metallic materials in corrosive media [7-63], especially, the plant

extracts act as inhibitor of steel in acid solution. Deng and Li [13] studied the corrosion inhibition of Ginkgo leaves extract for cold rolled steel in HCl and H_2SO_4 solutions, the results showed that the extract exhibited more efficient in 1.0 M HCl than in 0.5 M H_2SO_4. Garai et al. [15] reported that the corrosion inhibition effect of the crude methanolic extract of Artemisia pallens and the active component arbutin of Artemisia pallens on mild steel in 1 M HCl solution, the inhibition efficiencies were up to 98 % and 93 % respectively at the concentration of 400 mg/L, and the X-ray photoelectron spectroscopy confirmed the formation of inhibitor layer containing arbutin molecules, chloride and iron oxides. Oguzie and co-workers [22] found that the acid extract of leaves of Piper guineense effectively inhibited the corrosion of mild steel in acid solutions, and the results of quantum chemistry calculation about the key phytochemical constituents of the crude extract showed that piperine may be the most likely active component of the extract. From the foregoing, the corrosion inhibition performance of some plant extracts has been investigated, but compared with the huge number of plant resources and the potential demand for efficient green corrosion inhibitors, more research is still needed.

Houttuynia cordata (HC) is a native perennial herbaceous plant widely grown in the eastern and southern area of Asia, as a time-honored traditional Chinese medicine, HC has been associated with a variety of pharmacological activities such as antihypertension, antiviral, antileukemic, and antioxidative [64-67], and seems to have anticancer effects [66-67]. HC is found to be an important source of natural flavonoids and polysaccharides [65], and more than 30 compounds were isolated and identified from the HC extracts, including aristolactams, amides, flavonoids, benzenoids, and so on [68]. In the present study, the adsorption and inhibitive effect of acid extract of Houttuynia cordata (HCE) on the corrosion of mild steel in 0.5 M H_2SO_4 solution has been investigated through gravimetric measurement, electrochemical technique and topography examination.

2. EXPERIMENTAL

2.1. Electrolyte and Material

The corrosive medium of 0.5 M H_2SO_4 solution was prepared by dilution analytical grade sulphuric acid using distilled water. The chemical composition (in wt%) of mild steel used in the experiment as follows: C (0.16%), Si (0.18%), Mn (0.29%), P (0.014%), S (0.013%) and Fe for balance. A steel sample with diameter of 10 mm was used as working electrode for electrochemical measurement, the exposed surface area of working electrode was 0.785 cm^2, and its remainder was embedded by epoxy. The dimensions of specimens of gravimetric experiment and surface topography examination were 50 mm × 25 mm × 5 mm and 10 mm× 10 mm× 5 mm, respectively. Before the test, the specimens were sequentially polished using metallographic abrasive paper of 200 #, 400 #, 600 # and 800 #, then were rinsed with distilled water, degreased in acetone and dried at room temperature.

2.2. Preparation of Houttuynia cordata Extract (HCE) Solution

Houttuynia cordata (HC) were purchased from a vegetable market in Zigong in December 2014. In the experiment, the leaves of HC were removed, only its stem was retained. After cleaning and natural drying, HC was placed in the oven for drying 48 h at 50 ℃, then was ground to powder, and stored in a closed container. Stock solution of HCE was prepared as follows: 100 g of powdered HC were soaked in 1000 mL 0.5 M H_2SO_4 solution for 12 h, and then the residue was filtered out. The concentration of stock solution was determined to be 3 g/L by measuring the weight of the solution before and after extracting. Subsequently, the inhibited solutions with different concentrations including 0.15, 0.3, 0.75, 1.5 and 3 g/L were prepared through diluting the stock solution with appropriate quantity of 0.5 M H_2SO_4 solution.

2.3. Measurement Methods

Gravimetric experiments were conducted in a wild-mouth glass bottle. The test solution of 500 mL was put into the bottle, and was heated to the set temperature, and then 3 pieces of gravimetric analysis specimens and 2 pieces of topography monitoring samples were suspended in the bottle for 4 h. After that, the surface topography of the specimens was performed using a Tescan Vega3 scanning electron microscopy (SEM) at high vacuum. The gravimetric experiment procedures and the data processing steps have been reported earlier [4,69-70].

Electrochemical experiments were performed through the traditional three-electrode system using CHI660E electrochemical workstation (Shanghai Chenhua Instrument Co. Ltd.), in which the auxiliary electrode and reference electrode was the platinum electrode and saturated calomel electrode (SCE), respectively. Prior to measuring electrochemical impedance spectroscopy (EIS), the open circuit potential (OCP) of working electrode in test solution was monitored for 30 minutes, then EIS was measured using AC signals 5 mV peak to peak in the frequency range from 10^{-2} Hz to 10^{5} Hz. At last, the polarization curve was obtained by potentiodynamic scanning method in the potential range from -250 to +250 mV relative to OCP with a scan rate of 0.5 mV/s.

In all experiments, the test temperature was controlled by a constant temperature water bath with an accuracy of 1 K, and the test system was open to the air and under a static condition.

3. RESULTS AND DISCUSSION

3.1. Potentiodynamic Polarization Curves

Figure 1 shows the cathodic and anodic polarization curves of mild steel electrode in the absence and presence of various concentrations of HCE at 298 K. It can be found from Figure 1 the addition of HCE leads to the cathodic branch of the polarization curves significantly shift to the direction of low current density, and in which exist the Tafel linear region, but the nearly parallel cathodic polarization curves illustrate that HCE has little influence on the hydrogen reduction

mechanism. However, the anode current density does not decrease when adding low concentration of HCE, but even increases, until the HCE concentration is up to 0.3 g/L. And due to desorption of inhibitors, the anodic polarization curves are overlapped together when the polarization potential exceeds -0.35 V. Moreover, the Tafel linear region is not found on the anodic polarization curve. Thus, the electrochemical parameters, including corrosion potential (E_{corr}), corrosion current density (I_{corr}) and cathodic Tafel slope (β_c), are determined by Tafel extrapolation of the cathodic polarization curves to the E_{corr} [38], and are listed in Table 1. The inhibition efficiency (η) given in Table 1 is calculated according to the following equation:

$$\eta(\%) = (1 - \frac{I_{corr}}{I_{corr,0}}) \times 100 \quad (1)$$

where $I_{corr,0}$ and I_{corr} are the corrosion current density of mild steel electrode in the uninhibited and inhibited solutions, respectively.

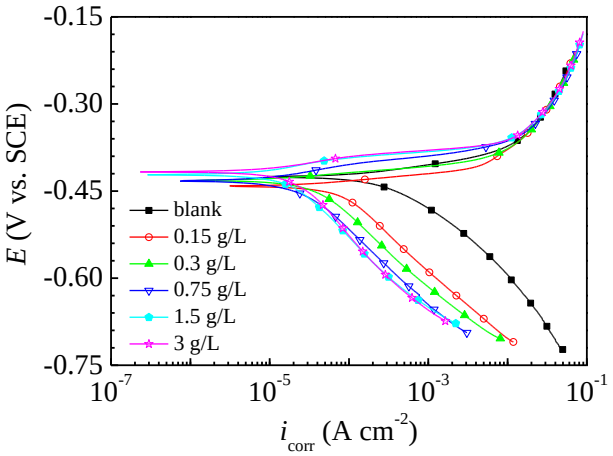

Figure 1. Potentiodynamic polarization curves for mild steel in 0.5 M H_2SO_4 solution without and with different concentrations of HCE at 298 K.

Table 1. The electrochemical parameters for mild steel in 0.5 mol/L H_2SO_4 solution without and with different concentrations of HCE at 298 K.

C(g/L)	E_{corr} (V vs. SCE)	I_{corr}(mA cm^{-2})	-β_c(mV dec^{-1})	η(%)	θ
blank	-0.425	0.3236	109.3	/	/
0.15	-0.441	0.0723	130.8	77.7	0.777
0.3	-0.432	0.0366	131.7	88.7	0.887
0.75	-0.433	0.0239	133.2	92.6	0.926
1.5	-0.422	0.0185	146.6	94.3	0.943
3	-0.412	0.0182	149.5	94.4	0.944

Table 1 show that the values of I_{corr} decrease with the increasing concentration of HCE, and the corrosion inhibition efficiency is accordingly improved. At the same time, the displacement in the change of corrosion potential is less than 20 mV, and the values of β_c are slightly changed, therefore, it can be thought that HCE is a mixed-type inhibitor with a predominantly cathodic action for mild steel in 0.5 M H_2SO_4 solution [49].

3.2. Electrochemical impedance spectroscopy (EIS)

Figure 2 shows the Nyquist and Bode plots of mild steel obtained in 0.5 M H_2SO_4 solution without and with different concentrations of HCE at 298 K. It can be seen from Figure 2(a) that the Nyquist plots are composed of a capacitive loop at high frequencies (HF) and an inductive loop at low frequencies (LF), and the addition of HCE has little influence on shapes of Nyquist plots and Bode plots, which indicate the presence of HCE dose not change the corrosion mechanism of mild steel in H_2SO_4 solution [10,26]. However, due to the adsorption of effective corrosion inhibitive constituents in extract, the diameter of capacitive loop significantly enhances with the increase of HCE concentration. Usually, the capacitive loop at HF is related to the charge transfer of the metal corrosion process and double layer behavior [42,49], and the LF inductive loop may be attributed to the adsorption-desorption of the intermediate species [47]. Bode plots in Figure 2(b) display a one time constant behavior, and the values of phase angle and impedance magnitude (|Z|) increase with the increasing of HCE concentration, which indicate better protection of inhibitor with higher concentrations [71].

According to the above analysis, the EIS is fitted to the equivalent circuit as shown in Figure 3 by ZSimpWin software, and the electrochemical impedance parameters are given in Table 2. In the circuit, R_S is the resistance of solution, L and R_L represent the inductive element and its corresponding resistance, respectively. R_{ct} is the charge transfer resistance, and due to the frequency dispersion caused by the imperfections of the electrode surface, constant phase element (CPE) is usually used to replace double layer capacitance (C_{dl}) [42,49], and CPE can be described as follows [42,49]:

$$Z_{CPE} = \frac{1}{Y_0(j\omega)^n} \quad (2)$$

where, Y_0 is the magnitude of CPE, j is the imaginary unit, ω is the angular frequency, and n is the phase shift. The C_{dl} values and inhibition efficiencies (η) are calculated according to the following equation [49,69]:

$$C_{dl} = Y_0(\omega_{max})^{n-1} = Y_0(2\pi f_{Z\,im\text{-}max})^{n-1} \quad (3)$$

$$\eta = \frac{R_{ct} - R_{ct,0}}{R_{ct}} \times 100 \quad (4)$$

where $R_{ct,0}$ and R_{ct} are the charge transfer resistance without and with inhibitor, respectively.

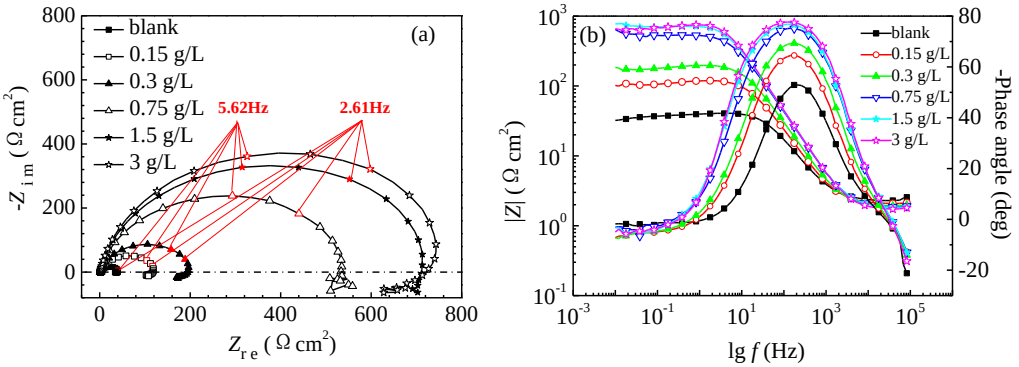

Figure 2. Nyquist plots (a) and Bode plots (b) for mild steel in 0.5 M H_2SO_4 solution without and with different concentrations of HCE at 298 K.

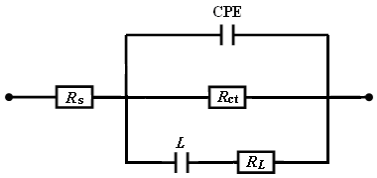

Figure 3. Equivalent circuits used to fit the EIS.

Table 2 shows that the values of R_{ct} increase, but the C_{dl} values decrease with the increasing HCE concentration, as a result, the inhibition efficiencies of HCE go up, which are attributed to the adsorption of effective constituents of HCE on the mild steel surface [42]. The values of *n* are close to one and the change is not significant, indicating the charge transfer process controls the dissolution mechanism of mild steel in test solution [42]. In addition, the inhibition efficiencies are in good agreement with those obtained from polarization curves.

Table 2. The EIS parameters for mild steel in 0.5 mol/L H_2SO_4 solution without and with different concentrations of HCE at 298 K.

C (g/L)	R_s (Ω cm^2)	$Y_0\times10^{-6}$ (S s^n cm^{-2})	*n*	R_{ct} (Ω cm^2)	C_{dl} (μF cm^{-2})	*L* (Ω cm^2)	R_L (Ω cm^2)	η (%)	θ
blank	2.4	183.9	0.88	33	95.2	2	6	/	/
0.15	2.1	137.0	0.89	100	83.3	16	21	67.0	0.670
0.3	2	98.2	0.90	163	63.7	40	35	79.8	0.798
0.75	1.9	63.8	0.92	481	48.0	128	64	93.1	0.931
1.5	1.9	58.6	0.93	602	46.3	399	135	94.5	0.945
3	1.8	54.4	0.93	635	43.0	120	154	94.8	0.948

3.3. Weight Loss Measurements

The results of gravimetric experiments for the corrosion of mild steel in 0.5 M H_2SO_4 solution in the absence and presence of the different concentrations of HCE for 4 h at 298 K are given in Table 3. It is clear that the corrosion rates decrease and the inhibition efficiencies increase with the increasing HCE concentrations, and when the concentration of HCE reaches 0.75 g/L, the inhibition efficiency is up to 90 %, which is in good agreement with the result obtained by electrochemical measurements.

Temperature is an important factor affecting the performance of corrosion inhibitor. Table 4 gives the corrosion parameters of mild steel in 0.5 M H_2SO_4 solution without and with 3 g/L of HCE for 4 h at different temperatures. The data shows the corrosion rates significantly increase with rising temperature, but the inhibition efficiencies are still more than 90%, which reflect HCE is an effective corrosion inhibitor of mild steel in 0.5 M H_2SO_4 solution.

In addition, the inhibition efficiency of HCE is compared with that of other plant extracts reported in literature [27,44,45,47,50], the related data are listed in Table 5. It can be seen that the

inhibition efficiency of HCE is slightly less than that of salvia officinalis leaves extract and tagetes erecta extract in 0.5 M H_2SO_4 solution, but higher than that of green tea extract, watermelon rind extract and strawberry fruit extract. Because the extraction methods and ingredients of plant extract are different, it is difficult to explain the differences in inhibition efficiency of different plant extracts, however, the data suggest that HCE is an effective inhibitor.

Table 3. Corrosion parameters obtained from weight loss measurement for mild steel in 0.5 M H_2SO_4 solution without and with different concentrations of HCE for 4 h at 298 K.

C(g/L)	v(g m^{-2} h^{-1})	η(%)	θ
blank	13.73	/	/
0.15	2.47	82.0	0.820
0.3	1.97	85.6	0.856
0.75	1.04	92.5	0.925
1.5	0.50	96.4	0.964
3	0.23	98.3	0.983

Table 4. Corrosion parameters of mild steel in 0.5 M H_2SO_4 solution without and with 3 g/L HCE for 4 h at different temperatures.

T(K)	C(g/L)	v(g m^{-2} h^{-1})	η(%)	θ
298	blank	13.73	/	/
	3	0.23	98.3	0.983
308	blank	21.21	/	/
	3	0.42	98.0	0.980
318	blank	41.00	/	/
	3	1.97	95.2	0.952
328	blank	58.38	/	/
	3	4.80	91.8	0.918

Table 5. The inhibition efficiency of HCE on the corrosion of steel in 0.5 M H_2SO_4 solution compared with that of other extract described in literature

Plant extract	C(g/L)	η(%)[1]	Test method[2]	Material	T(K)	Reference
HCE	0.3	85.6/79.8/88.7	WL/EIS/PDP	mild steel	298	this work
Salvia officinalis leaves extract	0.3	80.0/96.0	EIS/PDP	1018 carbon steel	298	[47]
Green tea extract	0.3	55.0/52.4/52.9	WL/EIS/PDP	carbon steel	303	[50]
Tagetes erecta extract	0.3	92.3/89.4/90.2	WL/EIS/PDP	mild steel	303	[27]
HCE	1.5	96.4/94.5/94.3	WL/EIS/PDP	mild steel	298	this work
Watermelon rind extract	1.5	73.93/75.57	EIS/PDP	mild steel	298	[44]
Strawberry fruit extract	1.5	77.3/69.8	EIS/PDP	mild steel	298	[45]

NOTE: [1] The inhibition efficiency was rounded off to three significant digits. [2] WL, EIS and PDP respectively represent the test methods of weight loss, electrochemical impedance spectroscopy and potentiodynamic polarization.

3.4. Thermodynamic and Kinetic Analysis

The above experimental results show that the corrosion inhibition of HCE is due to the adsorption of its effective ingredients on the surface of mild steel. In order to understand the interaction between the inhibitor and the mild steel surface, some adsorption isotherms are employed to fit the obtained experiment data. As a result, Figure 4 shows the plots of C/θ as function of θ are in a straight line, namely, the adsorption of HCE on metal surface obeys Langmuir adsorption isotherm. The isotherm is defined as equation 5 [36,41], in which, C is the concentration of HCE, K_{ads} is the adsorption equilibrium constant, θ is the surface coverage, its values have been given in the tables above. Moreover, the heat of adsorption (Q_{ads}) for the test system at HCE concentration of 3 g/L is calculated using the data in Table 4 by equation 6 [39,46], in which, R is the universal gas constant, and T is the thermodynamic temperature. The plots of $\ln(\theta/(1-\theta))$ vs. $1000/T$ yield a straight line as shown in Figure 5. Through the slope of the straight line, the calculated value of Q_{ads} is -47.50 kJ/mol, the negative value of Q_{ads} indicates that the adsorption of the inhibitor molecules on the surface of mild steel is exothermic process.

$$\frac{C}{\theta} = C + \frac{1}{K_{ads}} \quad (5)$$

$$\ln(\frac{\theta}{1-\theta}) = \ln A + \ln C - \frac{Q_{ads}}{RT} \quad (6)$$

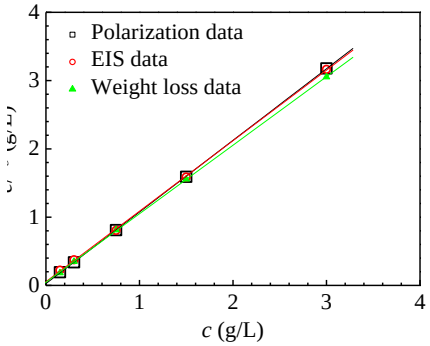

Figure 4. The Langmuir isotherm plots for mild steel in 0.5 M H_2SO_4 solution with different concentrations of HCE at 298 K.

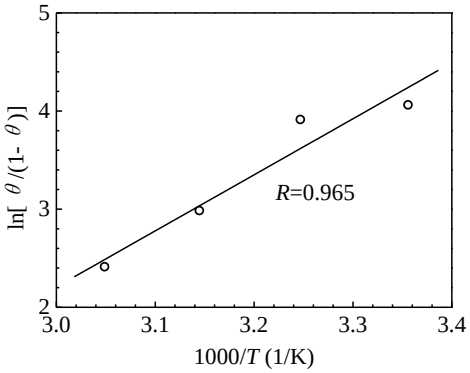

Figure 5. Plots of $\ln(\theta/(1-\theta))$ as function of $1000/T$ for mild steel in 0.5 M H_2SO_4 solution in the presence of 3 g/L HCE.

In order to further reveal the inhibition mechanism of HCE, the activation parameters for the corrosion process of mild steel in 0.5 M H_2SO_4 solution without and with 3 g/L HCE are calculated using the data in Table 4 through Arrhenius equation (7) and transition state equation (8) [36-37].

$$\ln \nu = -\frac{E_a}{RT} + \ln A \quad (7)$$

$$\ln \frac{\nu}{T} = \ln \frac{R}{Nh} + \frac{\Delta S_a}{R} - \frac{\Delta H_a}{RT} \quad (8)$$

where, E_a is the apparent activation energy, A is the pre-exponential factor, h is the Plank's constant, N is the Avogadro's number, ΔS_a and ΔH_a represent the apparent entropy and enthalpy of activation, respectively.

Figure 6 shows the Arrhenius plots and Transition state plots for mild steel in 0.5 M H_2SO_4 solution without and with 3 g/L HCE. Thus, the activation parameters are obtained through linear regression, and are listed in Table 6. Table 6 shows the activation energy of the reaction of mild steel in 0.5 M H_2SO_4 solution is lower than that in the presence of HCE, which suggest that the corrosion process of mild steel in the inhibited solution needs to overcome a higher energy barrier owing to the adsorption of inhibitive constituents.

Moreover, the positive values of ΔH_a demonstrate that the dissolution of mild steel in test solutions is an endothermic process, and the ΔH_a value increases with the addition of HCE, which means more energy is needed for the steel dissolution in the presence of HCE, as a result, the corrosion of mild steel is inhibited. Compared to the values of ΔS_a in Table 6, it is clear that ΔS_a is more positive in the presence of HCE than that in uninhibited solution, which indicates the disorderliness of the system is increased, and this phenomenon may be attributed to the replacement of water molecules adsorbed on the steel surface by the inhibitor molecules [36].

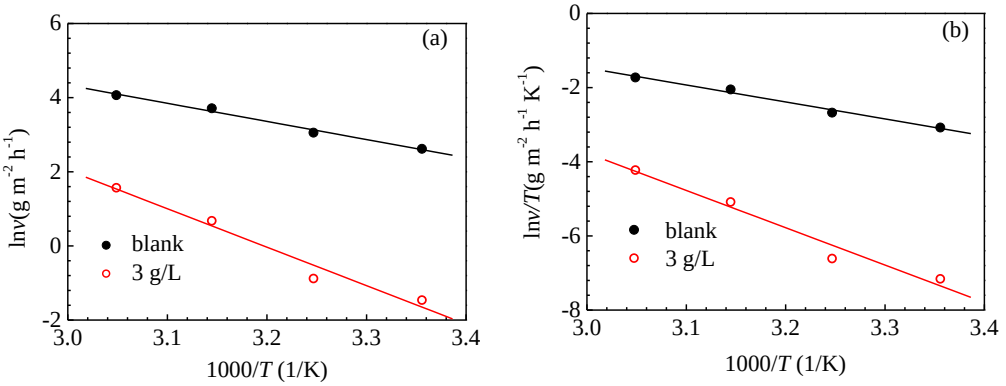

Figure 6. Arrhenius plots (a) and Transition state plots (b) for mild steel in 0.5 M H_2SO_4 solution without and with 3 g/L HCE.

Table 6. Activation parameters for mild steel in 0.5 M H_2SO_4 solution without and with 3 g/L HCE.

C(g/L)	E_a(kJ/mol)	ΔH_a(kJ/mol)	ΔS_a(J K^{-1} mol^{-1})
blank	40.66	38.06	-95.58
3	86.27	83.67	22.16

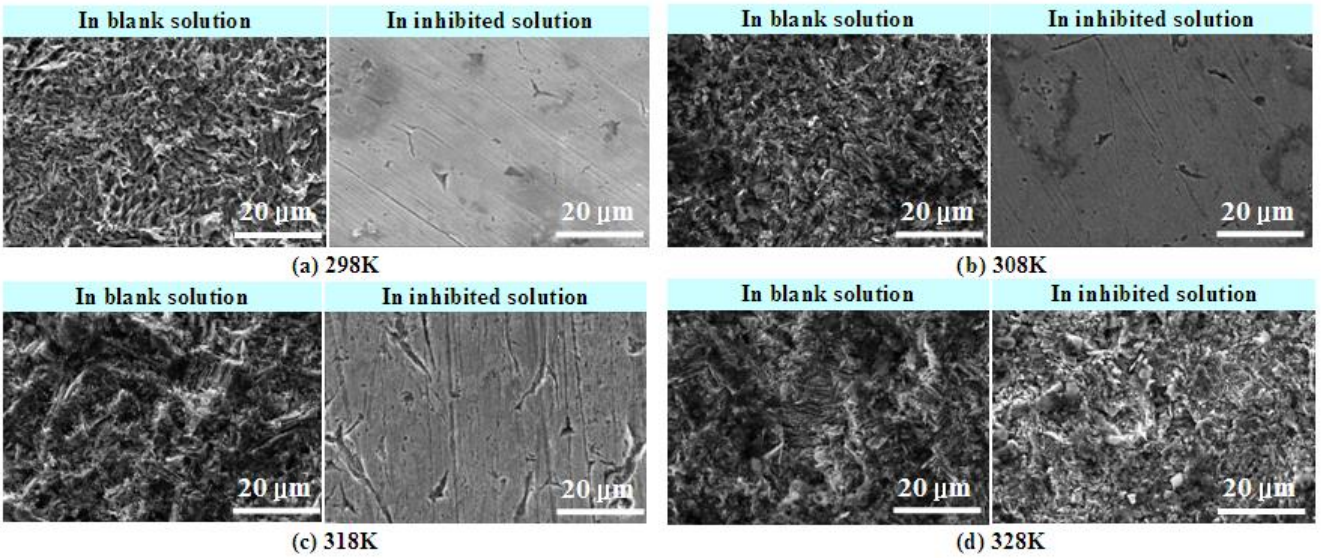

Figure 7. SEM micrographs of mild steel surface after immersed in 0.5 M H_2SO_4 solution in the absence and in presence of 3.0 g/L HCE for 4 h at different temperatures.

3.5. Surface Topography Examination

Figure 7 shows the SEM images of the mild steel samples immersed in 0.5 M H_2SO_4 solution without (blank solution) and with 3 g/L HCE (inhibited solution) for 4 h at different temperatures. It is clear that the surface of steel sample was seriously destroyed in blank solution due to the corrosion, however, in the inhibited solution, the corrosion phenomenon remains to be observed, but the damage degree of the surface is much lighter. Meanwhile, it can be seen that the damage is increased with increasing temperature, which is corresponded to the increase of the corrosion rate in weight loss experiment.

4. CONCLUSIONS

Houttuynia cordata acid extract (HCE) is a mixed-type inhibitor with a predominantly cathodic action for mild steel in 0.5 M H_2SO_4 solution, and exhibits good inhibition performance, its inhibition efficiency increases with the increase of the concentration of HCE, and when the concentration of HCE reaches 0.75 g/L, the inhibition efficiency is up to 90 % at 298 K. Although the inhibition efficiency of HCE is decreased with rising temperature but still up to 90 % at the concentration of 3 g/L under the test temperature (298 K to 328 K). The adsorption of HCE effective ingredients on the surface of mild steel leads to the increase in apparent activation energy of corrosion process, as a result, the corrosion of mild steel in H_2SO_4 solution is inhibited, and the adsorption is an exothermic process and obeys Langmuir isotherm.

ACKNOWLEDGMENTS
This project is supported financially by the Opening Project of Key Laboratory of Material Corrosion and Protection of Sichuan Province (No. 2016CL03) and Talent Project of Sichuan University of Science & Engineering (No. 2016RCL11).

References

1. J. Fu, H. Zang, Y. Wang, S. Li, T. Chen and X. Liu, *Ind. Eng. Chem. Res.*, 51 (2012) 6377.
2. E.E. Ebenso, M.M. Kabanda, L.C. Murulana, A.K. Singh and S.K. Shukla, *Ind. Eng. Chem. Res.*, 51 (2012) 12940.
3. R. Yıldız, A. Döner, T. Doğan and İ. Dehri, *Corros. Sci.*, 82 (2014) 125.
4. X. Zheng, S. Zhang, W. Li, L. Yin, J. He and J. Wu, *Corros. Sci.*, 80 (2014) 383.
5. J.C.D. Rocha, J.A.D.C.P. Gomes and E. D'Elia, *Corros. Sci.*, 52 (2010) 2341.
6. N. Soltani, N. Tavakkoli, M. Khayatkashani, M.R. Jalali and A. Mosavizade, *Corros. Sci.*, 62 (2012) 122.
7. S.A. Umoren, Z.M. Gasem and I.B. Obot, *Ind. Eng. Chem. Res.*, 52 (2013) 14855.
8. M. Bozorg, T.S. Farahani, J. Neshati, Z. Chaghazardi and G.M. Ziarani, *Ind. Eng. Chem. Res.*, 53 (2014) 4295.
9. L. Li, X. Zhang, J. Lei, J. He, S. Zhang and F. Pan, *Corros. Sci.*, 63 (2012) 82.
10. H. Gerengi and H.I. Sahin, *Ind. Eng. Chem. Res.*, 51 (2012) 780.
11. X. Li, S. Deng and H. Fu, *Corros. Sci.*, 62 (2012) 163.
12. T. Ibrahim, H. Alayan and Y.A. Mowaqet, *Prog. Org. Coat.*, 75 (2012) 456.
13. S. Deng and X. Li, *Corros. Sci.*, 55 (2012) 407.
14. U.M. Eduok, S.A. Umoren and A.P. Udoh, *Arab. J. Chem.*, 5 (2012), 325.
15. S. Garai, S. Garai, P. Jaisankar, J.K. Singh and A. Elango, *Corros. Sci.*, 60 (2012) 193.
16. S.S.D.A.A. Pereira, M.M. Pêgas, T.L. Fernández, M. Magalhães, T.G. Schöntag, D.C. Lago, L.F.D. Senna and E. D'Elia, *Corros. Sci.*, 65 (2012) 360.
17. M. Behpour, S.M. Ghoreishi, M. Khayatkashani and N. Soltani, *Mater. Chem. Phys.*, 131 (2012) 621.
18. H. Gerengi, K. Schaefer and H.I. Sahin, *J. Ind. Eng. Chem.*, 18 (2012) 2204.
19. N.O. Obi-Egbedi, I.B. Obot and S.A. Umoren, *Arab. J. Chem.*, 5 (2012), 361.
20. S. Deng and X. Li, *Corros. Sci.*, 64 (2012) 253.
21. M.A. Abu-Dalo, A.A.Othman and N.A.F. Al-Rawashdeh, *Int. J. Electrochem. Sci.*, 7 (2012) 9303.
22. E.E. Oguzie, C.B. Adindu, C.K. Enenebeaku, C.E. Ogukwe, M.A. Chidiebere and K.L. Oguzie, *J. Phys. Chem. C*, 116 (2012) 13603.
23. P.B. Raja, M. Fadaeinasab, A.K. Qureshi, A.A. Rahim, H. Osman, M. Litaudon and K. Awang, *Ind. Eng. Chem. Res.*, 52 (2013) 10582.
24. A.E. Bribri, M. Tabyaoui, B. Tabyaoui, H.E. Attari and F. Bentiss, *Mater. Chem. Phys.*, 141 (2013) 240.
25. I.E. Uwah, P.C. Okafor and V.E. Ebiekpe, *Arab. J. Chem.*, 6 (2013) 285.
26. X. Li, S. Deng, X. Xie and H. Fu, *Corros. Sci.*, 87 (2014) 15.
27. P. Mourya, S. Banerjee and M.M. Singh, *Corros. Sci.*, 85 (2014) 352.
28. X. Li, S. Deng, H. Fu and X. Xie, *Corros. Sci.*, 78 (2014) 29.
29. M.S. Al-Otaibi, A.M. Al-Mayouf, M. Khan, A.A. Mousa, S.A. Al-Mazroa and H.Z. Alkhathlan, *Arab. J. Chem.*, 7 (2014) 340.
30. N. Soltani, N. Tavakkoli, M. Khayat Kashani, A. Mosavizadeh, E.E. Oguzie and M.R. Jalali, *J. Ind. Eng. Chem.*, 20 (2014) 3217.
31. M. Chevalier, F. Robert, N. Amusant, M. Traisnel, C. Roos and M. Lebrini, *Electrochim. Acta*, 131 (2014) 96.
32. F. Suedile, F. Robert, C. Roos and M. Lebrini, *Electrochim. Acta*, 133 (2014) 631.

33. T. Ramde, S. Rossi and C. Zanella, *Appl. Surf. Sci.*, 307 (2014) 209.
34. K. Krishnaveni and J. Ravichandran, *J. Electroanal. Chem.*, 735 (2014) 24.
35. H.Z. Alkhathlan, M. Khan, M.M.S. Abdullah, A.M. Al-Mayouf, A.A. Mousa and Z.A.M. Al-Othman, *Int. J. Electrochem. Sci.*, 9 (2014) 870.
36. K. Boumhara, F. Bentiss, M. Tabyaoui, J. Costa, J.M. Desjobert, A. Bellaouchou, A. Guenbour, B. Hammouti and S.S. Al-Deyab, *Int. J. Electrochem. Sci.*, 9 (2014) 1187.
37. N.S. Patel, J. Hrdlicka, P. Beranek, M. Přibyl, D. Šnita, B. Hammouti, S.S. Al-Deyab and R. Salghi, *Int. J. Electrochem. Sci.*, 9 (2014) 2805.
38. A. Khadraoui, A. Khelifa, H. Boutoumi, H. Hamitouche, R. Mehdaoui, B. Hammouti and S.S. Al-Deyab, *Int. J. Electrochem. Sci.*, 9 (2014) 3334.
39. T.T. Bataineh, M.A. Al-Qudah, E.M. Nawafleh and N.A.F. Al-Rawashdeh, *Int. J. Electrochem. Sci.*, 9 (2014) 3543.
40. J.O. Okeniyi, C.A. Loto and A.P.I. Popopla, *Int. J. Electrochem. Sci.*, 9 (2014) 4205.
41. A.S. Fouda, S.H. Etaiw and W. Elnggar, *Int. J. Electrochem. Sci.*, 9 (2014) 4866.
42. A. Singh, Y. Lin, E.E. Ebenso, W. Liu, K. Deng, J. Pan and B. Huang, *Int. J. Electrochem. Sci.*, 9 (2014) 5585.
43. E. Rodriguez-Clemente, J.G. Gonzalez-Rodriguez and M.G. Valladares-Cisneros, *Int. J. Electrochem. Sci.*, 9 (2014) 5924.
44. N.A. Odewunmi, S.A. Umoren and Z.M. Gasem, *J. Ind. Eng. Chem.*, 21 (2015) 239.
45. S.A. Umoren, I.B. Obot and Z.M. Gasem, *Ionics*, 21 (2015) 1171.
46. S.N. Victoria, R. Prasad and R. Manivannan, *Int. J. Electrochem. Sci.*, 10 (2015) 2220.
47. A. Rodríguez-Torres, M.G. Valladares-Cisneros and J.G. Gonzalez-Rodríguez, *Int. J. Electrochem. Sci.*, 10 (2015) 4053.
48. A.Y.I. Rubaye, A.A. Abdulwahid, S.B. Al-Baghdadi, A.A. Al-Amiery, A.A.H. Kadhum and A.B. Mohamad, *Int. J. Electrochem. Sci.*, 10 (2015) 8200.
49. N. Soltani and M. Khayatkashani, *Int. J. Electrochem. Sci.*, 10 (2015) 46.
50. A.M. Alsabagh, M.A. Migahed, M. Abdelraouf and E.A. Khamis, *Int. J. Electrochem. Sci.*, 10 (2015) 1855.
51. M. Chellouli, D. Chebabe, A. Dermaj, H. Erramli, N. Bettach, N. Hajjaji, M.P. Casaletto, C. Cirrincione, A. Privitera and A. Srhiri, *Electrochim. Acta*, 204 (2016) 50.
52. N. Etteyeb and X.R. Nóvoa, *Corros. Sci.*, 112 (2016) 471.
53. H. Wang, M. Gao, Y. Guo, Y. Yang and R. Hu, *Desalination*, 398 (2016) 198.
54. A. Khadraoui, A. Khelifa, K. Hachama and R. Mehdaoui, *J. Mol. Liq.*, 214 (2016) 293.
55. M. Jokar, T.S. Farahani and B. Ramezanzadeh, *J. Taiwan Inst. Chem. Eng.*, 63 (2016) 436.
56. C. Rahal, M. Masmoudi, R. Abdelhedi, R. Sabot, M. Jeannin, M. Bouaziza and P. Refaitb, *J. Electroanal. Chem.*, 769 (2016) 53.
57. M. Prabakaran, S.H. Kim, V. Hemapriya, M. Gopiraman, I.S. Kim and I.M. Chung, *RSC Adv.*, 6 (2016) 57144.
58. S.P. Palanisamy, G. Maheswaran, C. Kamal and G. Venkatesh, *Res. Chem. Intermed.*, 42 (2016) 1.
59. Savita, P. Mourya, N. Chaubey, S. Kumar, V.K. Singh and M.M. Singh, *RSC Adv.*, 6 (2016) 95644.
60. S. Mo, H.Q. Luo and N.B. Li, *Chem. Pap.*, 70 (2016) 1131.
61. D.K. Verma and F. Khan, *Res. Chem. Intermed.*, 42 (2016) 3489.
62. I.A. Hermoso-Diaz, J.G. Gonzalez-Rodriguez and J. Uruchurtu-Chavarin, *Int. J. Electrochem. Sci.*, 11 (2016) 4253.
63. D.I. Njoku, I. Ukaga, O.B. Ikenna, E.E. Oguzie, K.L. Oguzie and N. Ibisi, *J. Mol. Liq.*, 219 (2016) 417.
64. W. Li, P. Zhou, Y. Zhang and L. He, *J. Ethnopharmacol.*, 133 (2011) 922.
65. L. Tian, Y. Zhao, C. Guo and X. Yang, *Carbohyd. Polym.*, 83 (2011) 537.

66. B.H. Cheng, J.Y. Chan, B.C. Chan, H.Q. Lin, X.Q. Han, X.L. Zhou, D.C. Wan, Y.F. Wang, P.C. Leung, K.P. Fung and C.B. Lau, *Carbohyd. Polym.*, 103 (2014) 244.
67. M.A. Kabir, T. Fujita, K. Ouhara, M. Kajiya, S. Matsuda, H. Shiba and H. Kurihara, *J. Dent. Sci.*, 10 (2015) 88.
68. S.C. Chou, C.R. Su, Y.C. Ku and T.S. Wu, *Chem. Pharm. Bull.*, 57 (2009) 1227.
69. X. Zheng, S. Zhang, M. Gong and W. Li, *Ind. Eng. Chem. Res.*, 53 (2014) 16349.
70. X. Zheng, S. Zhang, W. Li, M. Gong and L. Yin, *Corros. Sci.*, 95 (2015) 168.
71. A. Singh, A. Gupta, A.K. Rawat, K.R. Ansari, M.A. Quraishi and E.E. Ebenso, *Int. J. Electrochem. Sci.*, 9 (2014) 7614.